Magnetic field-induced assembly of oriented superlattices from maghemite nanocubes

Anwar Ahniyaz*†, Yasuhiro Sakamoto‡, and Lennart Bergström*§

*Materials Chemistry Research Group and ‡Division of Structural Chemistry, Department of Physical, Inorganic, and Structural Chemistry, Arrhenius Laboratory, Stockholm University, 10691 Stockholm, Sweden

Edited by Nicholas J. Turro, Columbia University, New York, NY, and approved September 17, 2007 (received for review May 6, 2007)

Tailoring the structure of nanocrystal superlattices is an important step toward controlled design of novel nanostructured materials and devices. We demonstrate how the long-range order and macroscopic dimensions of magnetic nanoparticle arrays can be controlled by the use of a modulated magnetic field. Inducing a dipolar attraction during the initial stage of the drying-mediated self-assembly process was sufficient to assemble the superparamagnetic oleate-capped maghemite nanocubes into large and defect-free superstructures with both translational and orientational order. The characteristic dimensions of the superlattice are controlled by the particle concentration as well as the duration of the applied magnetic field. The superparamagnetic maghemite nanocubes assemble into large and highly oriented thin arrays by applying the magnetic field perpendicular to the substrate surface only during the initial phase of drying-mediated self-assembly. Micrometer-sized and thick three-dimensional mesocrystals are obtained when the drying dispersion is subjected to an external magnetic field of moderate strength for the entire duration of the assembly process. The discovery of how translational and orientation order of nanocrystal superlattices can be induced by a temporal modulation of an anisotropic interparticle force offers new insight on the importance of the initial nucleation stage in the self-assembly process and suggests new routes for controlled self-assembly of dipolar nanocrystals.

mesocrystal | nanocrystal | nucleation | self-assembly | superparamagnetic

The assembly of nanoparticles into ordered superstructures is a generic phenomenon observed in materials of biological, geological, and man-made origin. Important examples include biomineralization (1) and ancient paints (2) and precipitates origination from slowly hydrolyzing aqueous solutions (3). The possibility to self-organize nanoparticles into two- and three-dimensional superlattices with a high degree of translational order has attracted much interest since the early observations of iron oxide "super crystals" (4). Indeed, understanding and optimizing the structures, at all length scales, of nanocrystal superlattices is an important step toward controlled design of novel nanostructured materials and devices. Arranging nanocrystals into ordered arrays and macroscopic structures with a specific packing arrangement has been used to engineer the band-gap of semiconductor quantum dot arrays (5) and high-density storage media (6, 7).

Mixing monodisperse spheres of different sizes and interactions can yield binary nanoparticle superlattices with a wide range of superstructures and tunable properties (8, 9). Although long-range translational order is essential, it is also of importance to attain a high degree of orientational order (10–13) to optimize, e.g., the magnetic properties (14). Indeed, oriented organization and attachment of nanocrystals is an important path for biomineralization processes (15, 16) to create materials with highly anisotropic mechanical properties.

Fundamentally, self-assembly into well defined structures requires that the colloidal building blocks have a well defined size and shape and that the interaction can be tuned to allow the system to attain a minimum free-energy state (17, 18). The range and magnitude of the attractive and repulsive interactions can also have a profound influence on the nucleation and growth rate and thus also the morphology and defect density of the nanocrystal superlattices. Rogach, Weller, and coworkers (19, 20) showed how a gradual destabilization through the slow diffusion of a poor solvent into the continuous phase of a dispersion of spherical nanocrystals can promote the formation of closely packed superlattices.

The possibility to tune the interactions of magnetic dipolar particles by an external field and thus control the clustering and transport properties has attracted a significant interest. The strong anisotropy of dipolar forces and the preference for a head-to-tail arrangement tend to promote the formation of chain-like clusters, but previous work has also shown how superparamagnetic nanoparticles can be assembled into clusters or larger superstructures (21, 22). We will show how the application of an external magnetic field on a dispersion of superparamagnetic maghemite nanocubes can induce the formation of defect-free superlattices with a very high degree of orientational order. It was possible to drastically alter the structure of the particle arrays from a mosaic-like pattern when no magnetic field was used to a superlattice with a very high degree of both translational and orientational order by subjecting the nanocube dispersion to a magnetic field of moderate strength for a short interval during the initial stage of the drying-mediated self-assembly process.

Results and Discussion

The truncated iron oxide nanocubes were produced by a modified nonhydrolytic synthesis approach (23). We found that the shape and size of the iron oxide nanocrystals could be controlled by the amount of the additional oleic acid (the iron-oleate:oleic acid molar ratio) and the heating rate. Although only spherical iron oxide nanocrystals were obtained at heating rates above 3°C/min, it was possible to synthesize exclusively cubic iron oxide nanoparticles when the heating rate was reduced to <2.6°C/min at an iron-oleate:oleic acid molar ratio of 3.5. The small but critical reduction in growth rate appears to promote the formation of iron oxide nanocrystals with a nonspherical, faceted shape. Fig. 1*A* shows a schematic representation of the truncated iron oxide nanocubes. The average edge length of the nanocube is 9 nm, which corresponds to a face diagonal length of 12.7 nm (assuming no truncation of the nanocube). The x-ray diffraction data [see supporting information (SI)] and the electron diffrac-

Author contributions: A.A. and L.B. designed research; A.A. and Y.S. performed research; A.A., Y.S., and L.B. analyzed data; and A.A., Y.S., and L.B. wrote the paper.

The authors declare no conflict of interest.

This article is a PNAS Direct Submission.

Abbreviation: TEM, transmission electron microscope/microscopy.

†Present address: Institute for Surface Chemistry, Drottning Kristinas Vag 45, 11486 Stockholm, Sweden.

§To whom correspondence should be addressed. E-mail: lennartb@inorg.su.se.

This article contains supporting information online at www.pnas.org/cgi/content/full/0704210104/DC1.

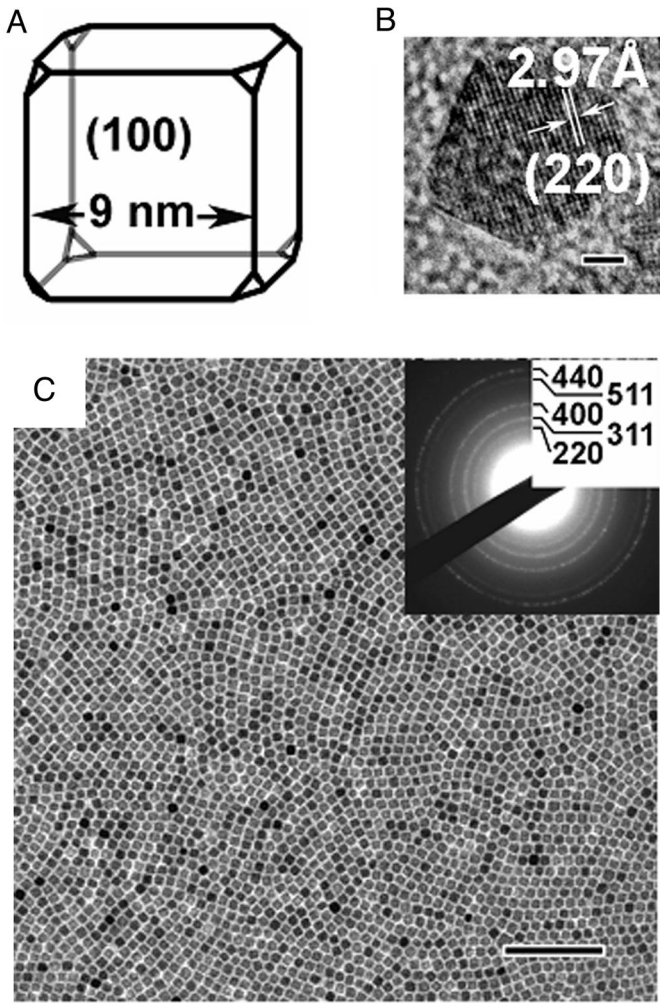

Fig. 1. Characterization and assembly of maghemite nanocubes. (*A* and *B*) A schematic representation (*A*) and high-resolution TEM image (*B*) of a {100} faceted, truncated maghemite nanocube. (Scale bar: 2 nm.) (*C*) TEM image and ED pattern (*Inset*) of a dense nanocube monolayer formed by drying at room temperature in the absence of an external magnetic field. (Scale bar: 100 nm.) The x-ray diffraction pattern of the nanocubes and the characterization of the magnetic properties can be found in the SI.

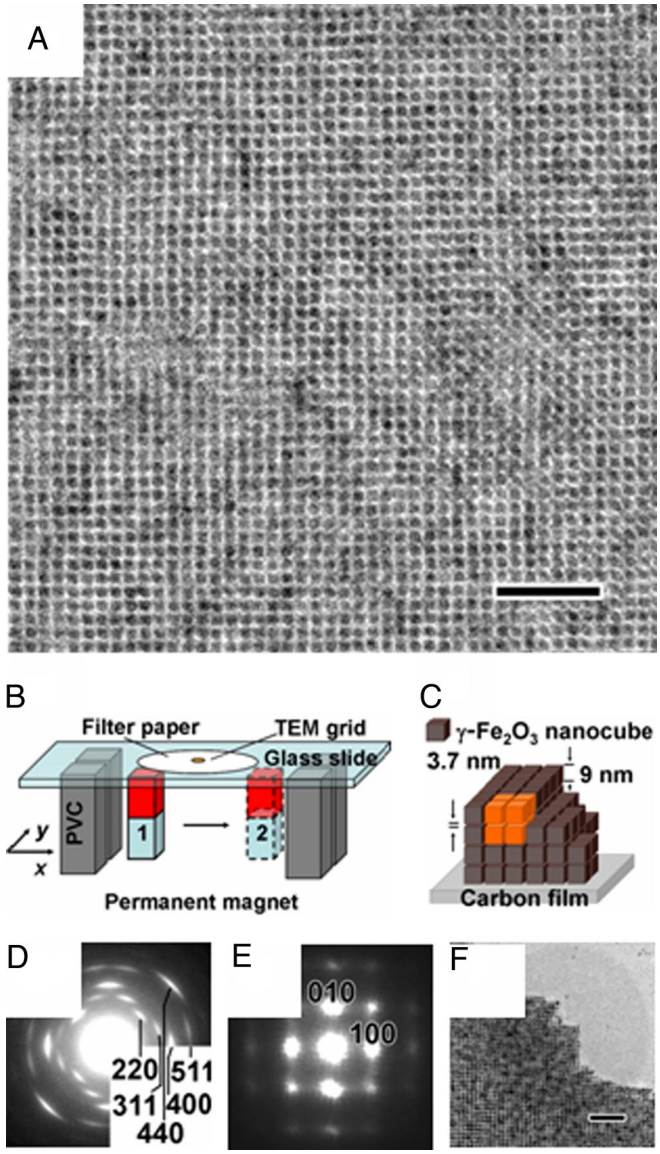

Fig. 2. Magnetic field-induced self-assembly of oriented superlattices from maghemite nanocubes. (*A*) TEM image of magnetic-field-induced self-assembly of maghemite nanocubes into an oriented superlattice. (Scale bar: 100 nm.) (*B*) Schematic presentation of the magnetic-field-induced self-assembly procedure. A single permanent magnet was first moved slowly from point 1 to point 2 and then moved in the orthogonal direction immediately (within 2 min) after one or several drops of the nanocube dispersion was placed onto the TEM grid. (*C*) A schematic representation of a simple cubic superlattice formed by magnetic-field-induced self-assembly. (*D* and *E*) Atomic (*D*) and mesoscale (*E*) electron diffraction patterns obtained from *A*. (*F*) TEM image obtained from the edge of the superlattice in *A*. (Scale bar: 100 nm.)

tion data (Fig. 1*C*) are consistent with a typical spinel structure (Fd-3m), characteristic for both maghemite (γ-Fe_2O_3, JCPDS no. 39-1346, S.G. $P4_132$, a = 8.3515 Å) and magnetite (Fe_3O_4, JCPDS no. 19-0629, S.G. Fd-3m, a = 8.396 Å). However, recent Mössbauer studies and isomer shift (δ) analysis have shown that the iron oxide nanocubes are predominantly maghemite (L. Häggström, S. Kamali, T. Ericsson, P. Nordblad, A.A., and L.B., unpublished observations). The high-resolution transmission electron microscopy (TEM) image (Fig. 1*B*) clearly shows the (220) lattice fringe of a crystal with a cubic symmetry along both face diagonal directions, i.e., the [220] and [−220] directions. The image contrast suggests that the sides of the truncated maghemite nanocubes are the {100} surfaces as shown in Fig. 1*A*.

The nanocubes can be assembled into mosaic-like particle arrays by simply placing a drop of the dilute toluene-based dispersion onto a suitable substrate, e.g., a TEM grid coated with amorphous carbon, and allowing the continuous liquid phase to evaporate. It is possible to form a dense monoparticulate array from a dispersion with an initial particle concentration of 4.2×10^{14} particles per milliliter and allow the particle monolayer to rearrange for a period of up to 2 weeks (Fig. 1*C*). Although the toluene evaporates within a short time, the nanocrystal dispersion also contains low-volatile additives like 1-octadecene and oleic acid, which provide the necessary fluidity of the wet particle monolayer to promote particle rearrangement into a densely packed configuration (24). The slow rearrangement and assembly produce local order within the monolayer; however, no long-range order or oriented attachment could be attained.

It is possible to drastically change the appearance of the final structure and create a highly ordered, virtually defect-free superlattice by subjecting the drying dispersion of the oleate-capped superparamagnetic maghemite nanocubes to a relatively

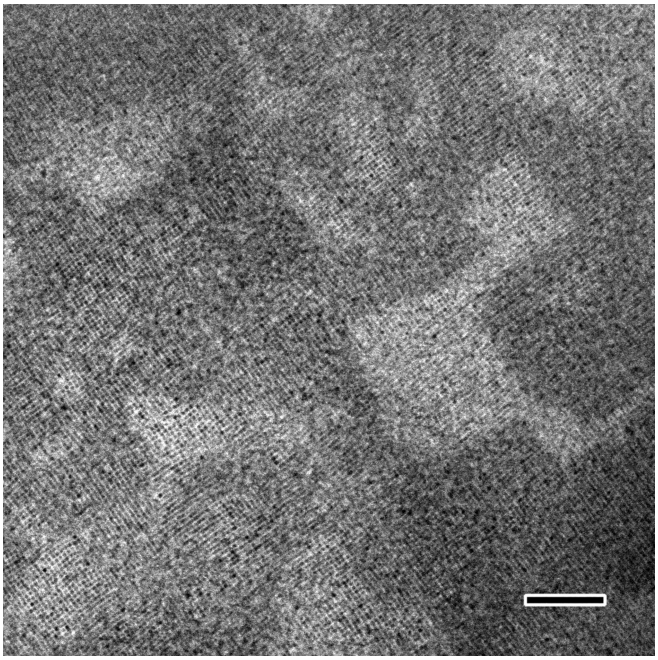

Fig. 3. TEM image of a section of a very large maghemite nanocube superlattice prepared by magnetic-field-induced self-assembly from a concentrated toluene-based dispersion of maghemite nanocubes. (Scale bar: 200 nm.) The contrast difference within the superlattice indicates that the different domains vary in layer thickness.

weak magnetic field for a very short period (<2 min) during the initial part of the slow assembly process (Fig. 2*A*). By slowly moving a permanent magnet, with the main-field axis directed perpendicular to the substrate surface, under the substrate immediately after the dispersion drop was applied (Fig. 2*B*), we were able to produce highly ordered superlattices with a typical dimension of up to several micrometers in the *x*–*y* plane and a thickness of a few particle monolayers. The permanent magnet that was used to modulate the magnetic field has a field strength that varies with position and distance. The maximum field strength close to the surface is $\|\vec{B}\| \leq 0.4$ T. We found that the magnetic-field-induced self-assembly was a relatively robust method to produce highly ordered superlattices of the cubic maghemite nanocrystals. Small variations in the distance between the magnet and surface of the substrate (and thus field strength) or in the speed of the movement did not have a discernible effect on the degree of order. The individual nanocubes are assembled into a simple cubic mesostructure. The constant separation distance of 3.7 nm corresponds to a slightly interdigitated oleate coating layer on the maghemite surfaces (Fig. 2*C*). The distinct texture of the diffraction pattern for the magnetically ordered superlattice (Fig. 2*D*) compared with the diffuse scattering rings for the monolayer produced in the absence of a magnetic field (Fig. 1*C*) suggest that the nanocubes are not only packed in regular fashion but also are crystallographically aligned. The single crystal-like diffraction spots of the electron diffraction pattern on the atomic scale (Fig. 2*D*) can be indexed corresponding to the [001] direction of maghemite. Indeed, the mesoscale electron diffraction pattern (Fig. 2*E*) shows that the crystallographic axes of superlattice mesostructure are identical to the orientation of individual maghemite nanocubes.

It is possible to produce nanocube superlattices with dimensions up to 10 μm, which by a conservative estimate contain $>10^6$ nanocubes, by careful control of the particle concentration and the drying time. Fig. 3 shows a section of such a large superlattice that can be obtained when several drops of the concentrated dispersion are placed on the substrate and allowed to dry for an extended time. It should be noted that these very large superlattices display some defects and dislocations. It may be possible to minimize these types of defects with the use of smoother substrates compared with the presently used TEM grids.

Fundamentally, the self-assembly process is controlled by the relative strength of van der Waals interaction, steric repulsion, and directional dipolar interactions together with possible substrate effects and space-filling consideration within the framework of drying-mediated self-assembly process (11, 13, 25). The intrinsic interactions (i.e., the sum of van der Waals attraction and steric repulsion in the absence of a magnetic field) between the maghemite nanocrystals in our system are apparently not of a sufficient magnitude to create a long-range translational or orientational order. However, a closer inspection of the mosaic-like array formed in the absence of a magnetic field (Fig. 1*A*) suggests that the nanocubes actually form small ordered clusters that fuse together into the large, disordered array that eventually forms by the drying-mediated process. Hence, it is possible that the dramatic change in the structure of the final superlattice that is obtained by subjecting the nanocube dispersion to a magnetic field only during the initial stage in the assembly process may be related to the nucleation and growth of such a cluster beyond a critical size. Hence, the additional field-induced attraction can promote the formation of a nucleus that is sufficiently large to dominate the subsequent growth of highly ordered orientation ordered colloidal crystal. The similarity of the jagged edge of the superlattice (Fig. 2*F*) to a single crystal grown from solution supports the conjecture that the superlattice grows by a slow crystallization process. Although the magnetic-field-induced dipole–dipole attraction between the individual superparamagnetic maghemite nanocrystals can be responsible for an alignment of the nanocubes, it is clear that also other attractive forces, e.g., the van der Waals attraction, must be responsible for the slow growth of large, highly ordered three-dimensional superlattices. Indeed, recent simulation studies have shown that it is necessary to consider both the dipolar and dispersive contributions when modeling the phase separation of ferrocolloids (26) and the rich phase diagram of semiconducting nanoparticles (27).

We find further proof of the delicate balance between the field-induced and intrinsic interaction between the nanocrystals from the ability of the superparamagnetic maghemite nanocubes to form large three-dimensional superlattices (mesocrystals) also when the magnetic field is applied during the entire duration of drying-mediated assembly process (Fig. 4*A*). The superlattices display a single crystal-like electron diffraction pattern (Fig. 4*B*), which suggests that also these thick three-dimensional superlattices or mesocrystals (28) have a high degree of orientational order, similar to the thin superlattices formed by the short time application of the external magnetic field. It was possible to control the thickness of the mesocrystals with the concentration of the nanoparticle dispersion and also to some extent with the strength of the magnetic field (see SI). If the concentration of the nanocube dispersion is very low, it becomes difficult to form a large continuous superlattice and several smaller arrays nucleate and grow (Fig. 4*C*). The high contrast of the individual nanocubes in the TEM image of Fig. 4*C* suggests that each array is very thin and that some parts of the assembly consist of only one particle layer. The small arrays are characterized by a high degree of order with some defects at the edges. Some arrays appear to have fused together at an angle, probably at a relatively late stage in the self-assembly process.

In summary, we have demonstrated how large maghemite nanocube superlattices with a high degree of crystallographic orientational order can be produced by a magnetic-field-induced

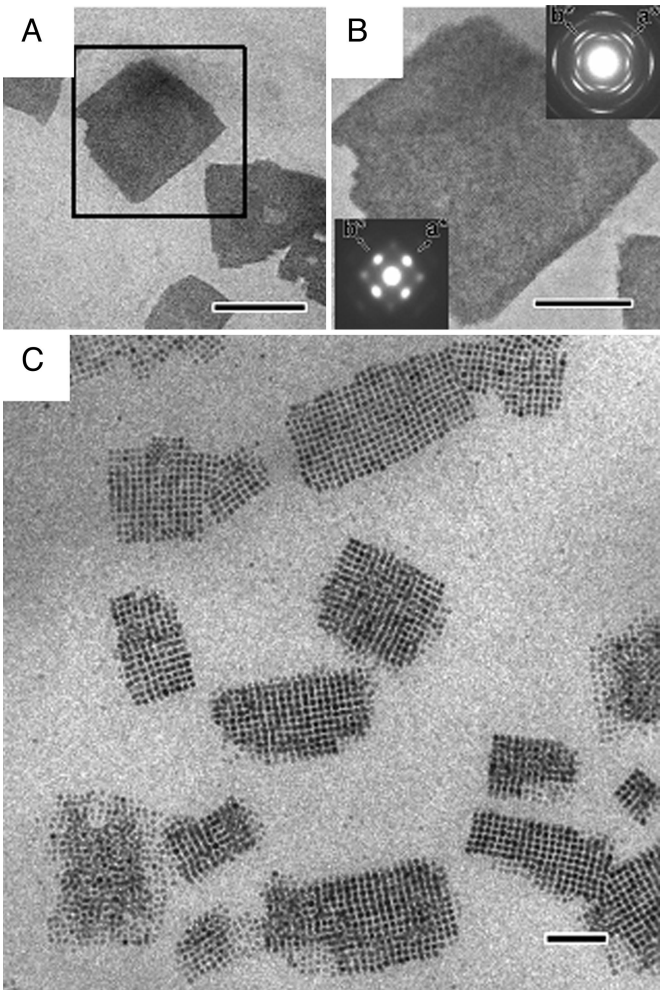

Fig. 4. Maghemite nanocube superlattices formed by slow drying of dilute and concentrated toluene-based dispersion of maghemite nanocubes under a constant magnetic field. (*A*) Low-magnification TEM image of superlattices formed from a concentrated (4.2×10^{14} particles per milliliter) nanocube dispersion. (Scale bar: 1 μm.) (*B*) Enlargement of a superlattice and selected area diffraction patterns on atomic scale (*Inset* in upper right) and mesoscale (*Inset* in lower left). (Scale bar: 500 nm.) (*C*) TEM image of the small nanocube arrays formed from a dilute (1.0×10^{14} particles per milliliter) toluene-based dispersion of maghemite nanocubes. (Scale bar: 100 nm.)

nucleation and growth self-assembly process. The strategy to induce a translational and orientational order of a superlattice of superparamagnetic maghemite nanocrystals by a temporal modulation of the dipolar interaction force not only may be extended to other superparamagnetic nanocrystals, but also could be used to tailor more complex structures from other systems that display directional, anisotropic interactions.

Materials and Methods

Synthesis and Separation of Iron Oxide Nanocrystals. The synthesis procedure is a modification of the nonhydrolytic thermal decomposition of iron-oleate in high-boiling organic solvent (23). The iron-oleate precursor was produced by reacting 10.8 g of iron chloride ($FeCl_3 \cdot 6H_2O$, 40 mmol, 98%; Aldrich) and 36.5 g of sodium oleate (120 mmol, 82%; Sigma–Aldrich) in a solvent mixture composed of 80 ml of ethanol, 60 ml of distilled water, and 140 ml of *n*-hexane. The mixture was refluxed at 70°C for 4 h, and the organic phase was collected and washed three times with 30 ml of distilled water. The remaining hexane in the organic phase was evaporated at 70°C leaving a dark brown iron-oleate residue.

In a typical synthesis procedure 36.5 g of iron-oleate (40 mmol) solid was dissolved in a mixture of 200 ml of 1-octadecene and ≈3.2–5.7 g (≈11.3–20 mmol) of oleic acid. The dissolved reactants and the reaction vessels were preheated in an oven at 100°C for 2 h to remove any trace amounts of water before the temperature was increased up to the reflux temperature at 320°C. The reaction was performed in air. The shape and size of the iron oxide nanocrystals could be controlled by the iron-oleate:oleic acid ratio and the heating rate. Truncated maghemite nanocubes were obtained when 3.2 g (11.3 mmol) of oleic acid was added (corresponding to an iron-oleate:oleic acid molar ratio of 3.5) and the system was slowly heated at 2.6°C/min to 320°C, where the mixture was refluxed for 30 min. Spherical maghemite nanocrystals were obtained when 5.7 g (20 mmol) of oleic acid was added (iron-oleate:oleic acid molar ratio of 2) and the system was heated at 3°C/min up to 320°C, where the mixture was refluxed for 30 min. We were able to separate the nanocrystals and obtain a concentrated dispersion of maghemite nanocrystals by ultracentrifugation of the as-prepared nanoparticle solution using a Beckman LK-80 ultracentrifuge. Centrifuging the as-synthesized nanocrystals at $300{,}000 \times g$ for 30 min at room temperature produces a black nanocrystal paste with 50 wt % solids content.

We have used three different concentrations of magnetite nanocube dispersions for the self-assembly experiments: one dilute (1×10^{14} particles per milliliter), one concentrated (4.2×10^{14} particles per milliliter), and one highly concentrated (8.4×10^{14} particles per milliliter). The dispersions were prepared by diluting the maghemite nanocube paste with a 50 wt % nanoparticle content in toluene, and simple hand-shaking was enough to redisperse the collected maghemite paste. The dispersions are virtually transparent with a dark brown color and remained stable over an extended time.

Self-Assembly in the Absence of an External Magnetic Field. Particle arrays were prepared by a drying-mediated self-assembly method. A few drops of a toluene-based dispersion of the maghemite nanocrystals were applied onto a carbon-coated Cu TEM grid that rests on a filter paper. The dispersion was allowed to slowly dry and assemble at room temperature for a period of ≈7–14 days.

Self-Assembly by Short-Time Exposure to External Magnetic Field. The superlattices were produced by the same drying-mediated process as described above, but the process was initiated by slowly moving a permanent magnet with the main-field axis directed perpendicular to the substrate surface under the substrate immediately after the dispersion drop was applied. The strength and direction of the magnetic field on the surface of this disk-shaped magnet were measured by a DC magnetometer (GM04 Gaussmeter; Hirst Magnetic Instruments, Cornwall, U.K.).

Formation of Superlattices by Slow Drying Under a Constant Magnetic Field. A drop of the maghemite nanocube dispersion in toluene was applied onto a carbon TEM grid and allowed to dry at room temperature for 1 week at room temperature under a weak magnetic field created by the same permanent magnet as was used for the spatiotemporal experiments. The field perpendicular to the substrate is significantly stronger that the field in the plane of the substrate.

Characterization. The x-ray diffraction patterns (see SI) of the separated maghemite paste were collected by using a PANalytical X'pert PRO diffractometer system with CuKα (λ = 0.1541 nm) at 45 V and 40 mA.

An MPMS2 SQUID magnetometer (Quantum Design, San Diego, CA) was used to study the magnetic properties of the separated maghemite nanocube paste (see SI).

Low- and high-resolution TEM images and electron diffraction patterns of maghemite nanocrystals were done by using a JEOL JEM-3010 microscope operating at 300 kV (Cs = 0.6 mm, point resolution 0.17 nm). The images were recorded with a CCD camera (size 1,376 × 1,032 pixels, pixel size 23.5 × 23.5 μm; model Keen View; SIS Analysis) at ×4,000–600,000 magnification.

We thank Dr. Andreas Fishers (Royal Institute of Technology of Sweden) for assistance with the powder XRD and L. Belova (Royal Institute of Technology of Sweden) for the SQUID measurements. This work was financially supported by the Swedish Research Council.

1. Cölfen H, Mann S (2003) *Angew Chem Int Ed* 42:2350–2365.
2. Jose-Yacaman M, Rendon L, Arenas J, Puche MCS (1996) *Science* 273:223–225.
3. Watson JHL, Cardell RR, Jr, Heller W (1962) *J Phys Chem* 66:1757–1763.
4. Bentzon MD, Van Wonterghem J, Moerup S, Thölen A, Koch CJW (1989) *Philos Mag B* 60:169–178.
5. Murray CB, Kagan CR, Bawendi MG (1995) *Science* 270:1335–1338.
6. Sun S, Murray CB, Weller D, Folks L, Moser A (2000) *Science* 287:1989–1992.
7. Zeng H, Li J, Liu JP, Wang ZL, Sun S (2002) *Nature* 420:395–398.
8. Shevchenko EV, Talapin DV, Kotov NA, O'Brien S, Murray CB (2006) *Nature* 439:55–59.
9. Cheon J, Park JI, Choi JS, Jun YW, Kim S, Kim MG, Kim YM, Kim YJ (2006) *Proc Natl Acad Sci USA* 103:3023–3027.
10. Dumestre F, Chaudret B, Amiens C, Renaud P, Fejes P (2004) *Science* 303:821–823.
11. Zheng RK, Gu HW, Xu B, Fung KK, Zhang XX, Ringer SP (2006) *Adv Mater* 18:2418–2421.
12. Song Q, Ding Y, Wang ZL, Zhang ZJ (2006) *J Phys Chem B* 110:25547–25550.
13. Redl FX, Black CT, Papaefthymiou GC, Sandstrom RL, Yin M, Zeng H, Murray CB, O'Brien SP (2004) *J Am Chem Soc* 126:14583–14599.
14. Harrell JW, Kang S, Jia Z, Nikles DE, Chantrell R, Satoh A (2005) *Appl Phys Lett* 87:202508/1–202508/3.
15. Heuer AH, Fink DJ, Laraia VJ, Arias JL, Calvert PD, Kendall K, Messing GL, Blackwell J, Rieke PC, Thompson DH (1992) *Science* 255:1098–1105.
16. Xu A-W, Antonietti M, Cölfen H, Fang Y-P (2006) *Adv Funct Mater* 16:903–908.
17. Whitesides GM, Grzybowski B (2002) *Science* 295:2418–2421.
18. Puntes VF, Krishnan KM, Alivisatos AP (2001) *Science* 291:2115–2117.
19. Talapin DV, Shevchenko EV, Kornowski A, Gaponik N, Haase M, Rogach AL, Weller H (2001) *Adv Mater* 13:1868–1871.
20. Shevchenko E, Talapin DV, Kornowski A, Wiekhorst F, Kötzler J, Haase M, Rogach A, Weller H (2002) *Adv Mater* 14:287–290.
21. Sahoo Y, Cheon M, Wang S, Luo H, Furlani EP, Prasad PN (2004) *J Phys Chem B* 108:3380–3383.
22. Legrand J, Ngo A-T, Petit C, Pileni M-P (2001) *Adv Mater* 13:58–62.
23. Park J, An K, Hwang Y, Park J-G, Noh H-J, Kim J-Y, Park J-H, Hwang N-M, Hyeon T (2004) *Nat Mater* 3:891–895.
24. Rabani E, Reichman DR, Geissler PL, Brus LE (2003) *Nature* 426:271–274.
25. Song Q, Zhang ZJ (2006) *J Phys Chem B* 110:11205–11209.
26. Ivanov AO, Novak EV (2007) *Colloid J* 69:302–311.
27. Talapin DV, Shevchenko EV, Murray CB, Titov AV, Kral P (2007) *Nano Lett* 7:1213–1219.
28. Cölfen H, Antonietti M (2005) *Angew Chem Int Edit* 44:5576–5591.